Electron Transport in a Methanofullerene**

By *Valentin D. Mihailetchi*, *Jeroen K. J. van Duren*, *Paul W. M. Blom*,* *Jan C. Hummelen*, *René A. J. Janssen*, *Jan M. Kroon*, *Minze T. Rispens*, *Wil Jan H. Verhees*, and *Martijn M. Wienk*

The current–voltage characteristics of methanofullerene [6,6]-phenyl C_{61}-butyric acid methyl ester (PCBM)-based devices are investigated as a function of temperature. The occurrence of space–charge limited current enables a direct determination of the electron mobility. At room temperature, an electron mobility of $\mu_e = 2 \times 10^{-7}$ $m^2 V^{-1} s^{-1}$ has been obtained. This electron mobility is more than three orders of magnitude larger than the hole mobility of donor-type conjugated polymer poly(2-methoxy-5-(3′,7′-dimethyloctyloxy)-*p*-phenylene vinylene) (OC_1C_{10}-PPV). As a result, the dark current in PCBM/OC_1C_{10}-PPV based devices is completely dominated by electrons. The observed field and temperature-dependence of the electron mobility of PCBM can be described with a Gaussian disorder model. This provides information about the energetic disorder and average transport-site separation in PCBM.

1. Introduction

Photovoltaic elements based on thin films of conjugated polymer/fullerene compounds are promising candidates for solar energy conversion.[1] Organic plastic solar cells have the potential for cost effectiveness. The mechanical flexibility and low specific weight of the plastic materials opens up a wide field of applications. A promising plastic solar cell candidate is based on the donor-type conjugated polymer poly(2-methoxy-5-(3′,7′-dimethyloctyloxy)-*p*-phenylene vinylene) (OC_1C_{10}-PPV) and acceptor molecules of [6,6]-phenyl C_{61}-butyric acid methyl ester (PCBM).[1]

As a concept, a bulk heterojunction that consists of a three-dimensional interpenetrating donor–acceptor network, sandwiched between two electrodes with different work functions, is used. This generates an electric field across the organic layer. For this kind of cells, a power conversion efficiency of 2.5 % under air mass (AM) 1.5 illumination has been reported.[2,3] From photophysical studies it has been demonstrated that after absorption of a photon, ultra-fast electron transfer takes place from the excited state of a conducting polymer to acceptor molecules such as Buckminster fullerenes (C_{60}), with a quantum efficiency close to unity.[4,5] Subsequently, the separated charge carriers are transported via the interpenetrating network to the electrodes. The photogenerated current is directly governed by the charge-carrier mobility, alongside the number of photoexcited charge carriers.

For the understanding of the opto-electronic properties of OC_1C_{10}-PPV/PCBM-based solar cells, knowledge about the charge transport properties of the individual components is indispensable. For OC_1C_{10}-PPV, the transport of holes has been extensively studied due to its application in polymer light-emitting diodes. From current density–voltage (*J*–*V*) measurements,[6] transient electroluminescent measurements,[7] and impedance spectroscopy,[8] a hole mobility μ_h of 5×10^{-11} $m^2 V^{-1} s^{-1}$ has been obtained for OC_1C_{10}-PPV. The field (*E*) and temperature (*T*) dependence of the hole mobility in PPV is described by a stretched exponential dependence

$$\mu(E,T) = \mu_0(T)\exp\left(\gamma(T)\sqrt{E}\right) \quad (1)$$

where $\mu_0(T)$ is the zero-field mobility and $\gamma(T)$ describes the field activation.[6–8]

In the present study, the electron transport in PCBM is investigated. It is demonstrated that the electron current in PCBM is space–charge-limited, which allows for a direct determination of the electron mobility μ_e from the *J*–*V* measurements. At room temperature, an electron mobility of 2×10^{-7} $m^2 V^{-1} s^{-1}$ is obtained. Consequently, at room temperature the electron mobility in PCBM is a factor of 4000 greater than the hole mobility in OC_1C_{10}-PPV, making OC_1C_{10}-PPV/PCBM bulk heterojunction solar cells electron-dominated devices.

Furthermore, it is demonstrated that the field- and temperature-dependence of μ_e also follows the empirical law $\mu \propto \exp(\gamma\sqrt{E})$. By analyzing the *E*- and *T*-dependence with a Gaussian disorder model, information about the microscopic charge transport in PCBM is obtained.

2. Results and Discussion

The devices under investigation consist of a single PCBM layer sandwiched between a hole-conducting layer of poly(3,4-ethylenedioxythiophene)/poly(styrene sulfonate) (PEDOT:PSS), typ-

[*] Prof. P. W. M. Blom, V. D. Mihailetchi, Prof. J. C. Hummelen, Dr. M. T. Rispens
Materials Science Centre, University of Groningen
Nijenborgh 4, NL-9747 AG Groningen (The Netherlands)
E-mail: P.W.M.Blom@phys.rug.nl
J. K. J. van Duren, Prof. R. A. J. Janssen, Dr. M. M. Wienk
Laboratory of Macromolecular and Organic Chemistry
Eindhoven University of Technology
PO Box 513, NL-5600 MB Eindhoven (The Netherlands)
Dr. J. M. Kroon, W. J. H. Verhees
Energy Research Centre of the Netherlands (ECN), Solar Energy
PO Box 1, NL-1755 ZG Petten (The Netherlands)

[**] These investigations were financially supported by the Dutch Ministries of EZ, O&W, and VROM through the EET program (EETK97115).

  1616-301X/03/0101-0043 $ 17.50+.50/0

ically of 100 nm thickness, and an evaporated lithium fluoride (LiF) (~1nm)/aluminum (Al) (~40nm) top electrode (see Experimental). In the inset of Figure 1, an energy band diagram of the device is shown under flat-band conditions.

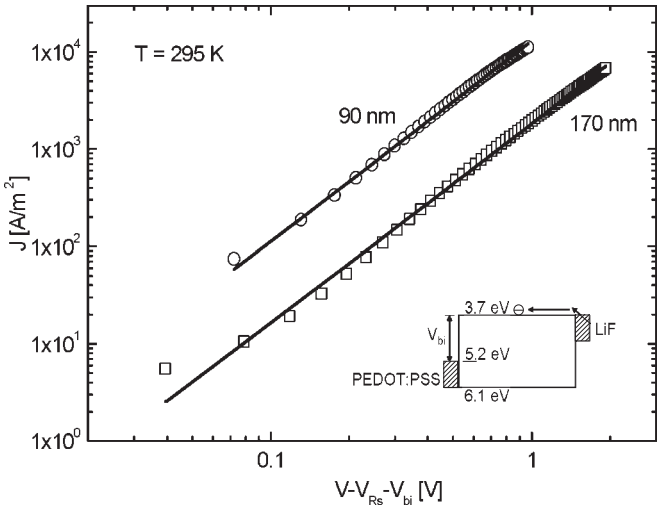

Fig. 1. Experimental (symbols) and calculated (solid lines) *J–V* characteristics of ITO/PEDOT:PSS/PCBM/LiF/Al devices with thickness $L = 90$ nm and 170 nm, using $V_{bi} = 1.4$ eV and $R_s = 30\ \Omega$. The device band diagram is indicated in the inset. The electron transport is described by SCLC (Equation 2) with an electron mobility $\mu_e = 2.0 \times 10^{-7}\ m^2\,V^{-1}\,s^{-1}$ and a dielectric constant $\varepsilon_r = 3.9$.

From the work functions, it is expected that LiF will form an Ohmic contact for electron injection on PCBM. The work function of PEDOT:PSS (5.2 eV) does not match the highest occupied molecular orbital (HOMO) level of PCBM (6.1 eV),[1] thus hole injection from PEDOT:PSS into PCBM can be neglected. Consequently, only electrons are expected to flow in the PCBM under forward bias conditions.

Furthermore, from the energy band diagram at room temperature, a built-in voltage V_{bi} of around 1.5 V is expected. The *J–V* measurements were performed in a nitrogen atmosphere within a temperature range of 150–300 K. With decreasing temperature V_{bi} is expected to typically increase by 0.3 eV in the range 300–150 K, due to diffusion of thermally injected charges.[9] The active area amounts to 10^{-5} m^2. In Figure 1, the experimental *J–V* characteristics at room temperature (295 K) are shown for PCBM devices with layer thicknesses, *L*, of 90 nm and 170 nm.

Using $V_{bi} = 1.4$ V it is observed from the slope of the log(*J*) versus log(*V*) plot that the current density depends quadratically on the voltage. This behavior is characteristic for space–charge limited current (SCLC), and is described by[10]

$$J = \frac{9}{8}\varepsilon_0\varepsilon_r\mu_e\frac{V^2}{L^3} \tag{2}$$

where $\varepsilon_0\varepsilon_r$ is the permittivity of PCBM. From capacitance–voltage measurements we have obtained a relative dielectric constant ε_r of 3.9 for PCBM. Using $\varepsilon_r = 3.9$, we find that the *J–V* characteristics of our devices with $L = 90$ and 170 nm are well described by Equation 2, with $\mu_e = 2 \times 10^{-7}\ m^2\,V^{-1}\,s^{-1}$. Thus the observation of SCLC provides direct information on the electron mobility in PCBM. It should be noted that for current densities larger than 1000 A m^{-2}, the applied voltage should be corrected for the voltage drop across the indium tin oxide (ITO) series resistance V_{Rs}, which typically amounts to 25–30 Ω in our substrates. An important conclusion is that at room temperature, the electron mobility of PCBM is a factor of 4000 greater than the hole mobility of OC_1C_{10}-PPV. As a result, in a bulk heterojunction solar cell the photo-generated electrons in the PCBM are much more mobile than the holes in the OC_1C_{10}-PPV. Furthermore, in a bulk heterojunction solar cell, OC_1C_{10}-PPV and PCBM are typically used at a weight ratio of 1:4.[1] Due to this weight ratio, the OC_1C_{10}-PPV is heavily diluted, and that fact might further increase the mobility difference in an actual solar cell. The observed electron mobility of $2 \times 10^{-7}\ m^2\,V^{-1}\,s^{-1}$ in PCBM is a factor of 40 less than mobilities reported from field-effect measurements on thin films of evaporated C_{60}, which are typically $8 \times 10^{-6}\ m^2\,V^{-1}\,s^{-1}$.[11] For C_{60} single-crystals grown from the vapor phase, mobilities of $5 \times 10^{-5}\ m^2\,V^{-1}\,s^{-1}$ have been measured by time-of-flight experiments.[12] The reduction of the mobility in PCBM films as compared to C_{60} single crystals indicates that disorder may play an important role in PCBM thin films.

Figure 2 shows the *J–V* characteristics of a PCBM device with $L = 170$ nm as a function of temperature. In order to describe the electron current in PCBM, the SCLC model is

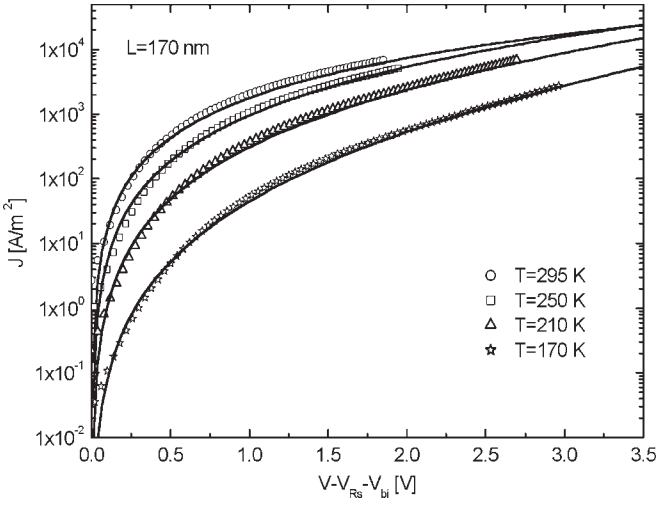

Fig. 2. Experimental (symbols) *J–V* characteristics of an ITO/PEDOT:PSS/PCBM/LiF/Al device with thickness $L = 170$ nm for various temperatures. Also shown are the calculated *J–V* characteristics (lines) as predicted by a SCLC model using the field dependent mobility defined by Equation 1.

combined with the field-dependent mobility of Equation 1. The *J–V* characteristics of the PCBM device are now characterized by the following equations[10]

$$J = en(x)\mu_n(E(x))E(x) \tag{3}$$

$$\frac{\varepsilon_0\varepsilon_r}{e}\frac{dE(x)}{dx} = n(x) \tag{4}$$

where $n(x)$ is the density of electrons at position x. Assuming Ohmic contacts ($x = 0$), we have the boundary condition

  1616-301X/03/0101-0044 $ 17.50+.50/0

ADVANCED FUNCTIONAL MATERIALS

$n(0) = N_c$, where the effective density of states in the conduction band, $N_c = 2.5 \times 10^{19}$ cm^{-3}.[6] Equations 1, 3, and 4 can be solved numerically for a given electron current density. The voltage is given by

$$V = \int_0^L E(x)\mathrm{d}x \tag{5}$$

The built-in voltage V_{bi} has been gradually increased from 1.4 eV (295 K) to 1.7 eV (150 K).[9] From Figure 2 it appears that the dependences of E and T on the J–V characteristics are consistently described by the combination of SCLC and the empirical mobility given by Equation 1. This demonstrates that the empirical mobility from Equation 1 is also applicable to the electron transport in PCBM.

This empirical mobility appears to be generic for a large class of disordered materials[13] such as molecularly doped polymers, pendant-group polymers, conjugated polymers, and organic glasses. This suggests that the conduction mechanisms in these various material systems are identical. It has been demonstrated from Monte Carlo simulations that hopping between sites that is subject to positional and energetic disorder reproduces the stretched exponential field dependence of the empirical mobility (Eq. 1).[14] In these calculations, the site energy distribution is assumed to be Gaussian, characterized by a width, σ. This Gaussian density of states (DOS) reflects the energetic spread in the transport sites due to disorder. Taking into account long-range spatial energy correlation improves the agreement between the simulations and the empirical $\mu \propto \exp(\gamma\sqrt{E})$ behavior at low electric fields.[15]

Such energy-correlation may originate from charge–dipole interactions in the material. From these simulations, a mobility of the following form has been proposed

$$\mu = \mu_\infty \exp\left[-\left(\frac{3\sigma}{5k_B T}\right)^2 + 0.78\left(\left(\frac{\sigma}{k_B T}\right)^{3/2} - 2\right)\sqrt{\frac{eaE}{\sigma}}\right] \tag{6}$$

where μ_∞ is the mobility as the limit $T \to \infty$, σ is the width of the Gaussian DOS, a is the intersite spacing, and k_B is Boltzmann's constant. From the J–V characteristics as shown in Figure 2, the temperature-dependence of μ_0 and γ (Eq. 1) is determined. According to Equation 6, the slope of a plot of the zero-field mobility $\mu_0 \sim T^{-2}$ then directly provides a value for σ. In Figure 3, the experimental μ_0 is plotted against T^{-2}. For $\sigma = 0.073$ eV, the predictions of the disorder model are in excellent agreement with the experimental electron mobilities.

Subsequently, with σ known from the slope of $\gamma \sim T^{-1.5}$ the intersite distance, a, can be determined. As shown in Figure 4, the experimental γ is consistently described by using an intersite distance of 3.4 nm. From the same analysis as that applied to the hole mobility of OC_1C_{10}-PPV, $\sigma = 0.11$ eV, and $a = 1.2$ nm have been reported.[16] The lower thermal activation and resulting smaller σ of PCBM as compared to OC_1C_{10}-PPV, demonstrates that the energetic disorder is significantly smaller in PCBM, which gives rise to a higher mobility. In conjugated polymers like OC_1C_{10}-PPV the energetic disorder will be enhanced by fluctuations in the length of the transporting conjugated chain segments. The obtained average site-separation of

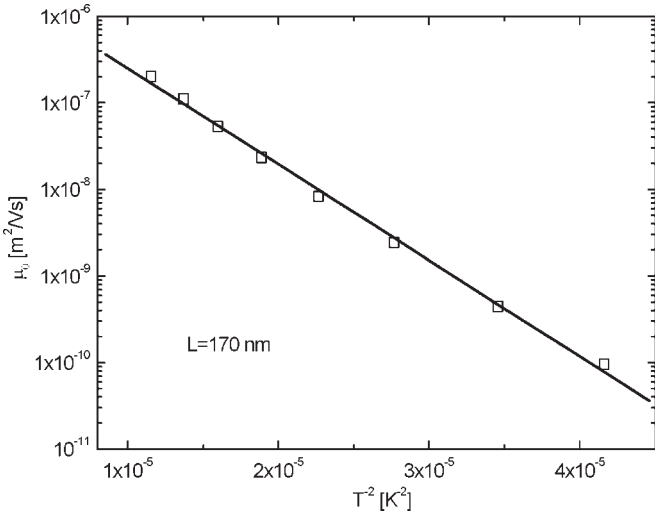

Fig. 3. Temperature dependence of the zero-field mobility μ_0 of PCBM from the J–V characteristics shown in Figure 2. The data are fitted with the $\ln(\mu_0) \sim T^{-2}$ law for hopping transport in a Gaussian DOS (Equation 6). The energy width σ of the DOS amounts to 0.073 eV.

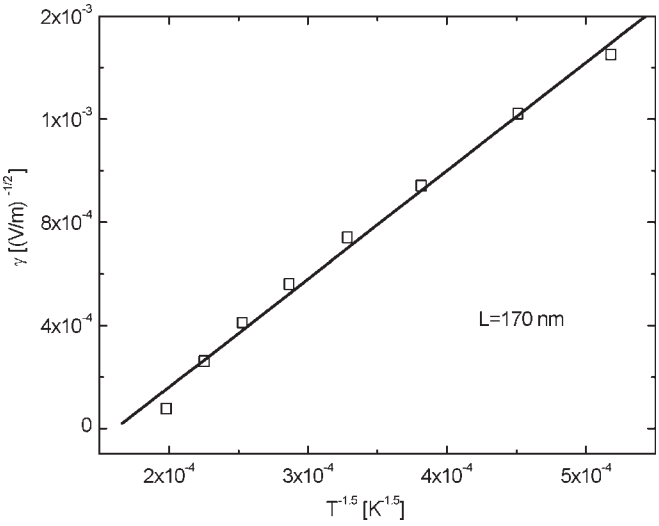

Fig. 4. Temperature dependence of the field activation coefficient γ as obtained from the J–V characteristics shown in Fig. 2. The solid line represents the calculated γ according to the disorder model (Equation 6), using an average site distance of 3.4 nm.

the PCBM transporting sites (3.4 nm) is larger than the diameter of the PCBM molecule (typically 1 nm). The relation to the morphology of pure PCBM thin films, which at present is not known, is a subject of further investigation.

3. Conclusions

In conclusion, the electron transport in PCBM has been studied by means of J–V measurements. At room temperature, the PCBM electron mobility exceeds the hole mobility of OC_1C_{10}-PPV by more than three orders of magnitude. The field and temperature dependence of the electron mobility of PCBM is described by the empirical law $\mu \propto \exp(\gamma\sqrt{E})$. Comparing the

  1616-301X/03/0101-0045 $ 17.50+.50/0

E and *T* dependence of the PCBM mobility with the correlated Gaussian disorder model provides information on the microscopic transport parameters. The enhanced electron mobility of PCBM as compared to the hole mobility in OC_1C_{10}-PPV is due to less energetic disorder in PCBM.

4. Experimental

Devices were prepared as follows. The ITO-covered glass substrates were first cleaned by ultrasonic treatment in acetone, rubbing with soap, rinsing with demineralized water, refluxing with isopropanol, and finally by UV–ozone treatment. Subsequently, a layer of PEDOT:PSS (Bayer AG) was spin-coated from an aqueous dispersion under ambient conditions onto the cleaned substrates, and the layer was dried by annealing the substrate. Next, the layer of PCBM was spin-coated on a Chemat Technology spin-coater (model KW-4A) at 1500 rpm from a chlorobenzene solution on top of the PEDOT:PSS layer, and the sample was transferred to an N_2 atmosphere glove box. Finally, a ~1 nm LiF layer and a ~100 nm Al protecting layer were deposited by thermal evaporation under vacuum (5×10^{-6} mbar, 1 ppm O_2 and <1 ppm H_2O). Organic film thickness measurements were performed with a Tencor P10 surface profiler. *J–V* curves were measured with a Keithley 2400 Sourcemeter in an Oxford Optistat continuous flow, exchange gas cryostat.

Received: July 8, 2002
Final version: August 20, 2002

[1] C. J. Brabec, N. S. Sariciftci, J. C. Hummelen, *Adv. Funct. Mater.* **2001**, *11*, 15.
[2] S. E. Shaheen, C. J. Brabec, N. S. Sariciftci, F. Padinger, T. Fromherz, J. C. Hummelen, *Appl. Phys. Lett.* **2001**, *78*, 841.
[3] J. M. Kroon, M. M. Wienk, W. J. H. Verhees, J. C. Hummelen, *Thin Solid Films* **2002**, *403*, 223.
[4] N. S. Sariciftci, L. Smilowitz, A. J. Heeger, F. Wudl, *Science* **1992**, *258*, 1474.
[5] C. J. Brabec, G. Zerza, G. Cerullo, S. De Silvestri, S. Luzati, J. C. Hummelen, N. S. Sariciftci, *Chem. Phys. Lett.* **2001**, *340*, 232.
[6] P. W. M. Blom, M. J. M. de Jong, M. G. van Munster, *Phys. Rev. B: Condens. Matter* **1997**, *55*, R656.
[7] M. C. J. M. Vissenberg, P. W. M. Blom, *Synth. Met.* **1999**, *102*, 1053.
[8] H. C. F. Martens, H. B. Brom, P. W. M. Blom, *Phys. Rev. B: Condens. Matter* **1999**, *60*, R8489.
[9] G. G. Malliaras, J. R. Salem, P. J. Brock, J. C. Scott, *J. Appl. Phys.* **1998**, *84*, 1583.
[10] M. A. Lampert, P. Mark, *Current Injection in Solids*, Academic Press, New York **1970**.
[11] R. C. Haddon, A. S. Perel, R. C. Morris, T. T. M. Palstra, A. F. Hebard, R. M. Fleming, *Appl. Phys. Lett.* **1995**, *67*, 121.
[12] E. Frankevich, Y. Maruyama, H. Ogata, *Chem. Phys. Lett.* **1993**, *214*, 39.
[13] P. M. Borsenberger, D. S. Weiss, *Organic Photoreceptors for Imaging Systems*, Dekker, New York **1993**.
[14] H. Bässler, *Phys. Status Solidi* **1993**, *B175*, 15.
[15] S. V. Novikov, D. H. Dunlap, V. M. Kenkre, P. E. Parris, A. V. Vannikov, *Phys. Rev. Lett.* **1998**, *81*, 4472.
[16] H. C. F. Martens, P. W. M. Blom, H. F. M. Schoo, *Phys. Rev. B: Condens. Matter* **2000**, *61*, 7489.

  1616-301X/03/0101-0046 $ 17.50+.50/0